Report
for the Stardust Cratering Group

MPI for Chemistry Mainz
(P. Heck, P. Hoppe, J. Huth)

June 15, 2006

SEM/EDX investigations of craters in Stardust Al foils

C2013N
C2037N
C2044W
C2052N
C2126W

Contents

List of Tables:

List of Figures:

MPI Mainz Stardust team

Philipp Heck, heck@mpch-mainz.mpg.de
Peter Hoppe, hoppe@mpch-mainz.mpg.de
Joachim Huth, huth@mpch-mainz.mpg.de

1. Analysis overview

Table 1 gives an overview of the analyses made on craters in Al foils 013N, 037N, 044W, 052N, 086N, and 126W. The SEM/EDX work on the large crater in Al foil 086N was done by Anton Kearsley at NHM; only the NanoSIMS analyses were made at MPI. The SEM/EDX data on this foil are thus not included in this report.

Table 1: Analysis overview for craters in Al foils 013N, 037N, 044W, 052N, 086N, and 126W.

Foil	Large[1] crater?	Systematic crater search by SEM	# craters analyzed by EDX	# craters analyzed by NanoSIMS	Additional information
013N	yes	-	EDX scanning of large crater	1	Progr. Rep. Isotope Group, 16.06.06
037N	-	yes	20	-	-
44W	-	yes	13	10	Progr. Rep. Isotope Group, 26.04.06;
052N	-	yes	35	31	Progr. Rep. Isotope Group, 26.04.06;
086N	yes	-	-	1	Progr. Rep. Isotope Group, 16.06.06; Progr. Report by A. Kearsley
126W	-	yes	-	-	-

[1] >10 µm.

2. Crater Statistics

Four Al foils (037N, 044W, 052N, 126W) were scanned for the presence of craters by SEM (Leo 1530 FESEM). In a first step the foils were completely scanned with a resolution sufficient to identify craters > 2 μm. Only one crater in this size range was found on foil 037N (crater #1, 3.8 μm). In a second step, systematic (automated) scans with pixel resolution of 130 nm (110 nm on foil 037N) were made on selected regions of all foils (Fig. 1); this permits to identify craters with sizes > ~200 nm (rim-to-rim, ~300 nm for outer boundary of lip). Scanned areas were 1.4 mm^2 (037N), 5.5 mm^2 (044W), 9.0 mm^2 (052N), and 5.2 mm^2 (126W). This resulted in the identification of 240 craters (Figs. 2 and 3a-d, Table 2, Appendix A); additional 6 craters <2 μm were found during a random search (not included in Figs. 3a-d and Table 2), i.e., a total of 247 craters was identified. There is large variation in crater density between foils, possibly a hint for large-scale clustering: 0.4 craters/mm^2 (126W), 3.3 craters/mm^2 (044W), 18.4 craters/mm^2 (052N), and 38.6 craters/mm^2 (037N). Crater sizes are between 110 nm and 1.8 μm (Table 3), except for the "big" one identified during the low-magnification survey of foil 037N (3.8 μm, Fig. 2). In a representation of crater density vs. crater size the data points of craters with sizes between 350 nm and 2 μm fall approximately (though slightly higher) on the extension of the line defined by craters with sizes > 20 μm (Fig. 4). There is a sharp decrease in crater density for craters with sizes smaller than 350 nm; this might be an observational bias or might be real.

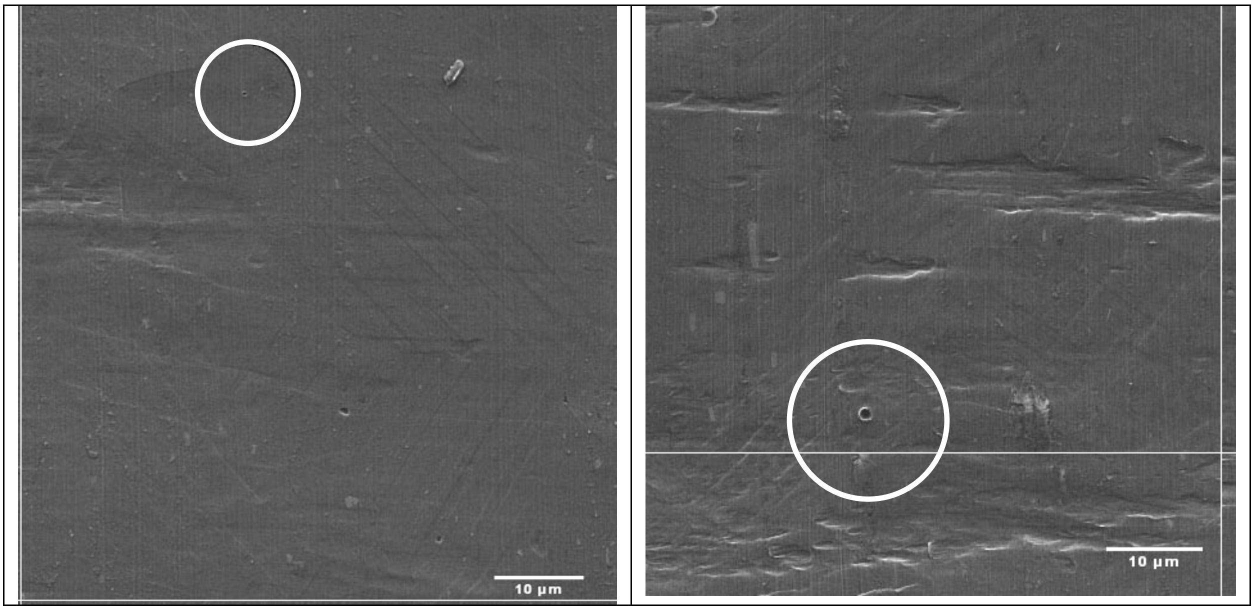

044W, Crater 11	**044W, Crater 13**

Figure 1: Two examples for crater recognition by the systematic scanning of Al foil 044W with pixel resolution of 130 nm.

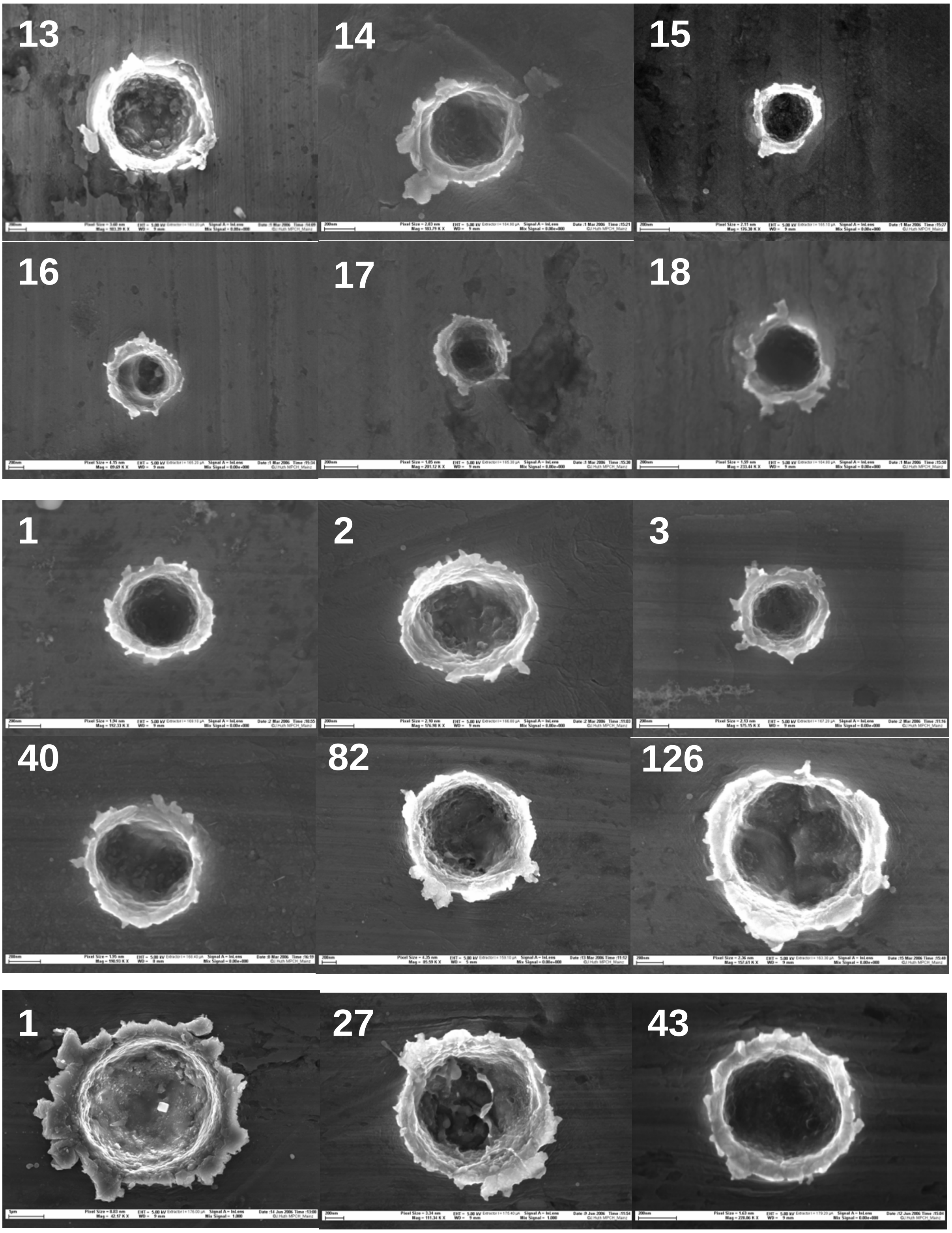

<u>Figure 2:</u> SEM images of selected craters in Al foils 044W (two top rows), 052N (two middle rows), and 037N (bottom row). The numbers indicate the crater number in Appendix A (Craters 1, 2, and 3 in 052N are not listed in the Appendix because they were found in a random search).

Figure 3a: Craters on Al foils 037N (left half). The yellow-shaded areas were systematically scanned for the presence of craters with sizes > ~200 nm. The locations of craters are indicated by red dots. Dito in Figs. 3b-d. The coordinates of the craters and of the corners of scanned fields are given in Appendix A.

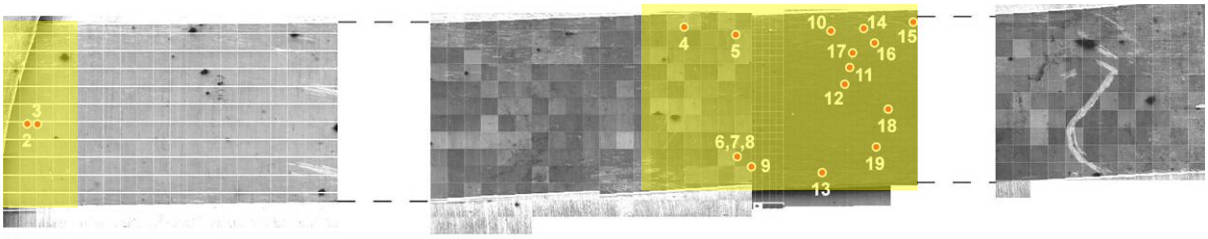

Figure 3b: Craters on Al foil 044W.

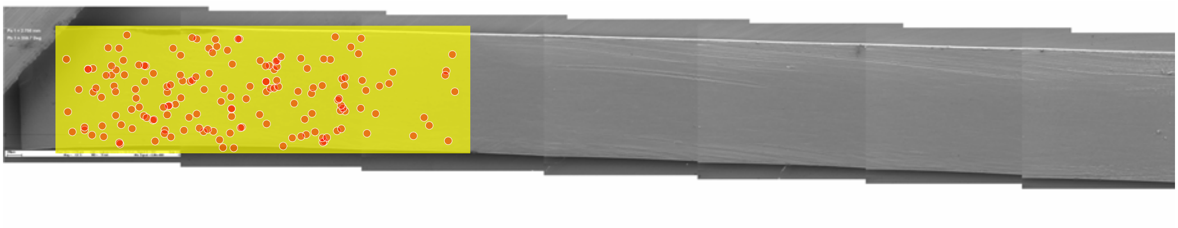

Figure 3c: Craters on Al foil 052N (left half).

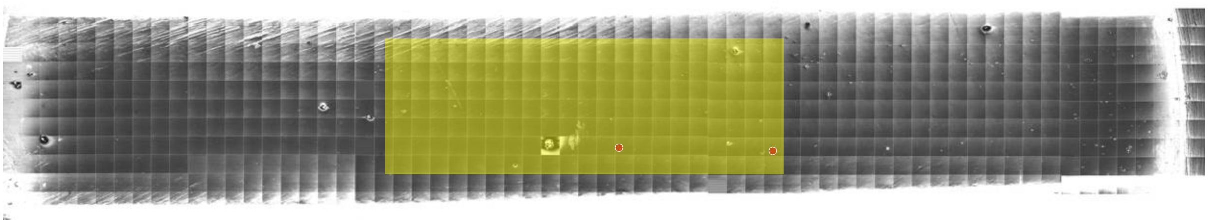

Figure 3d: Craters on Al foil 126W.

Table 2: Crater data summary (from the systematic high-resolution scans).

Foil	Scanned area (mm^2)	Identified craters	Crater density (mm^{-2})
037N	1.4	54	38.6
44W	5.5	18	3.3
052N	9.0	166	18.4
126W	5.2	2	0.4
Total	21.1	240	11.4

Table 3: Crater size distribution.

Size bin (µm)	# Craters (037N)	# Craters (044W)	# Craters (052N)	# Craters (126W)	# Craters (Total)	Crater density ($10^5/m^2$)
1.76-2.65	1	0	0	0	1	0.47
1.17-1.76	1	0	5	0	6	2.84
0.78-1.17	4	1	7	0	12	5.69
0.52-0.78	12	4	21	0	37	17.5
0.35-0.52	16	5	67	1	89	42.2
0.23-0.35	16	5	54	1	76	36.0
0.15-0.23	4	3	8	0	15	7.11
0.10-0.15	0	0	4	0	4	1.90

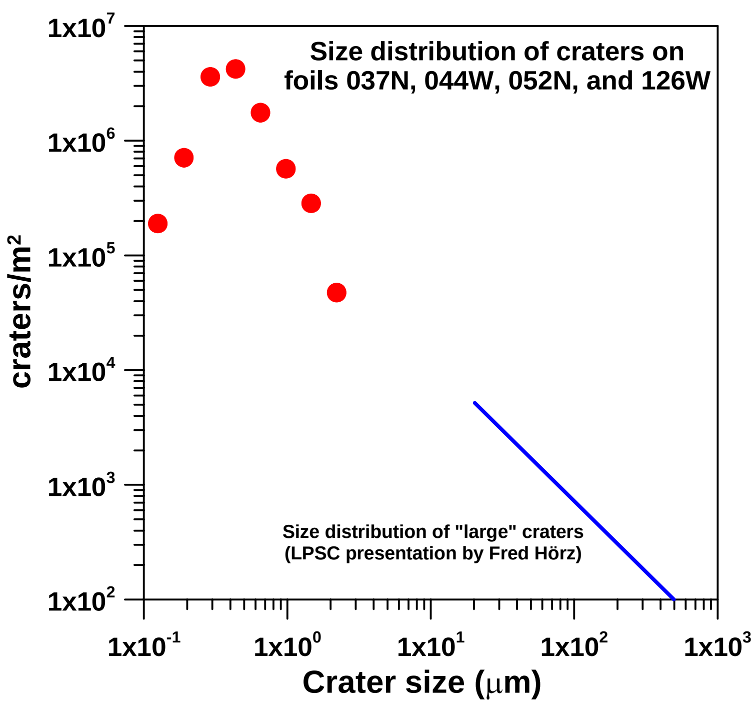

Figure 4: Crater size distribution (red symbols: this work; blue line: LPSC presentation by Fred Hörz).

3. EDX analyses of crater residues

3.1. EDX calibration

EDX calibration measurements were done on Admire Olivine (Fo88) and Phyrrhotite ($Fe_{0.83-1}S$). EDX acquisition and data reduction was made with the INCA software from Oxford Instruments. Two types of samples were prepared and studied at 5 and 20 kV: (i) Stardust-type Al foils which were bombarded with Admire Olivine and Pyrrhotite at a velocity of ~6 km/s (provided by Anton Kearsley). (ii) Polished sections of grains from both samples.

The measurements on the polished sections revealed only small differences (~5-6 % relative error) for Mg and Si between the measurements at 5 kV and 20 kV. For Fe the calculated abundances at 5 kV resulted in an abundance some 70% higher than that obtained at 20 kV. Larger differences are observed between the residues in small (<2 μm) craters and the polished sections. There is also significant scatter from crater to crater. If we take the 20 kV measurements on the polished olivine sample as reference for Mg, Si, and Fe then the crater data acquired at 5 kV (used for the small Stardust craters) should be corrected by factors of 1.15 (Mg), 0.99 (Si), and 0.49 (Fe). For S the situation appears somewhat more complicated because some fraction of the volatile S might have been evaporated during Phyrrhotite impact on the foil and the 20 kV measurement on the polished sample might not be a good reference. Instead we determined a S/Fe correction factor from a comparison of the measurements on crater residues made at 20 kV and 5 kV. This factor was calculated to be 1.63. These correction factors are included in the numbers (the element abundances were re-normalized to give 100% for the total) given for the Stardust crater residues in Appendix B. In view of the general difficulties with the quantification at 5 kV and for residues inside small craters we will not try to determine the detailed mineralogy of residues but will just divide the EDX patterns into three basic types.

A background measurement of the Al foil indicated variable Fe contents (see the EDX map of foil 013N in Fig. 7); Fe concentrations in the Stardust crater residues should thus be considered only upper limits.

3.2. Foils 044W and 052N

A total of 48 craters (13 from foil 044W, 35 from foil 052N) was analyzed by EDX (5 kV, integral, 100 s, ISIS software). Useful EDX data were obtained for 26 craters (160 nm – 1.5 μm). For the small samples and the experimental setup used here (ISIS) we are not able to give quantitative element abundances. However, the EDX spectra of 24 out of 26 craters can be qualitatively divided into three patterns, one of type FeS (type I) and two of type silicate (low and high S, types II and III) (Figs. 5a-c). The EDX spectra of the remaining two craters are dominated by C (and O) and Fe, respectively.

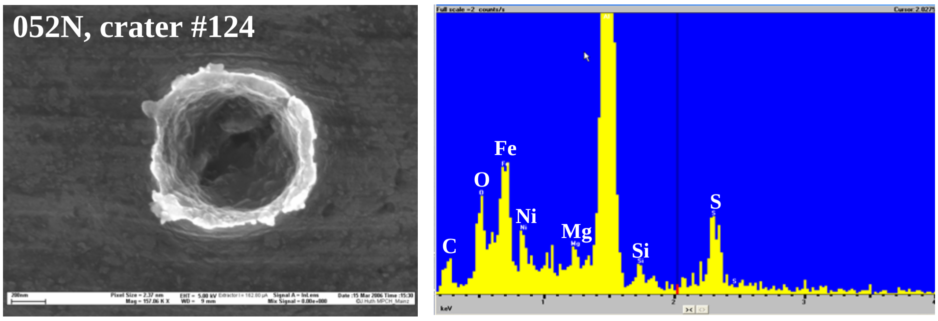

<u>Figure 5a:</u> SEM image and EDX spectrum of crater 052N-124 as an example for the EDX pattern I: FeS-type with small (variable) amounts of Mg, Si and Ni (6 out of 24 craters).

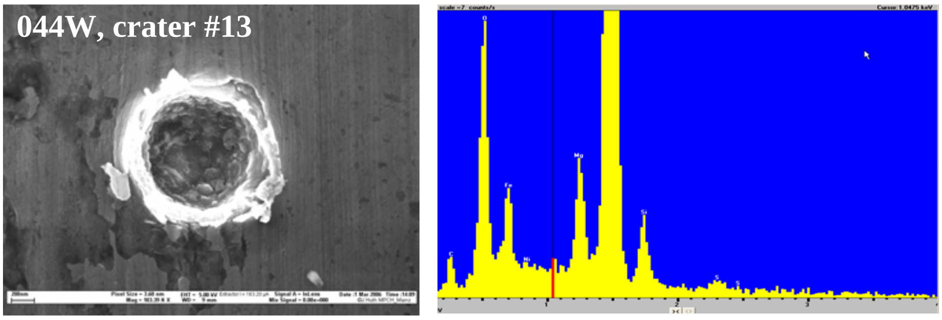

<u>Figure 5b:</u> SEM image and EDX spectrum of crater 044W-13 as an example for the EDX pattern II: Silicate-type, variable Mg/Si, low S (7 out of 24 craters).

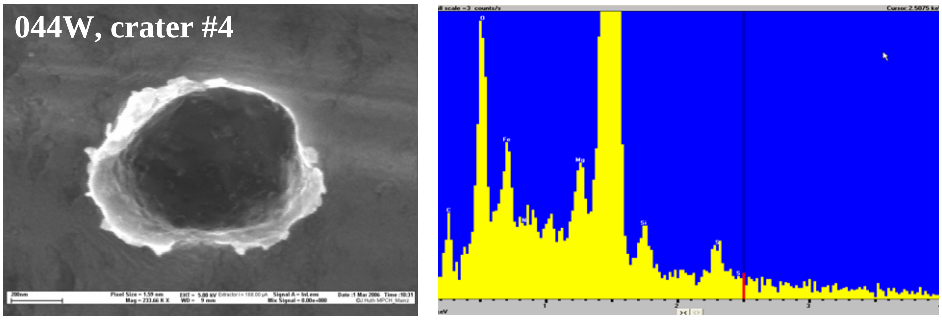

<u>Figure 5c:</u> SEM image and EDX spectrum of crater 044W-4 as an example for the EDX pattern III: Silicate-type, variable Mg/Si, relatively high S (11 out of 24 craters).

3.3. Foil 037N

Twenty craters were studied by EDX (5 kV, spot, 100 s, INCA software), 19 of which gave useful EDX data. Examples of selected spectra are shown in Fig. 6. The calculated element abundances are given in Appendix B but they should be taken only with care (see above). According to the classification scheme given in section 3.2, 3 craters are of type I, 8 of type II, and 8 of type III.

Figure 6a: EDX spectrum of crater 037N-12 as an example for the EDX pattern I: FeS-type (3 out of 19 craters).

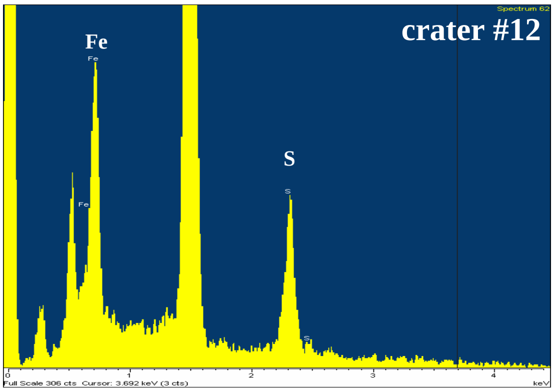

Figure 6b: EDX spectrum of crater 037N-4 as an example for the EDX pattern II: silicate-type, variable Mg/Si, low S (8 out of 19 craters).

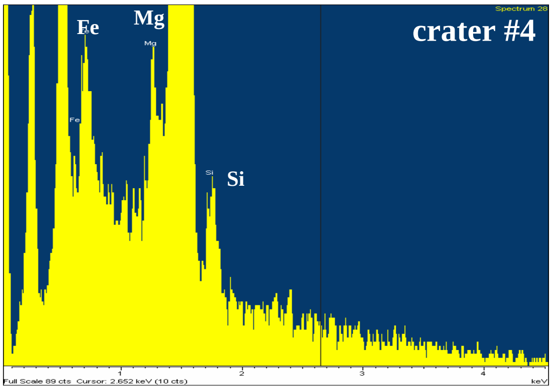

Figure 6c: EDX spectrum of crater 037N-56 as an example for the EDX pattern III: Silicate-type, varibale Mg/Si, relatively high S (8 out of 19 craters).

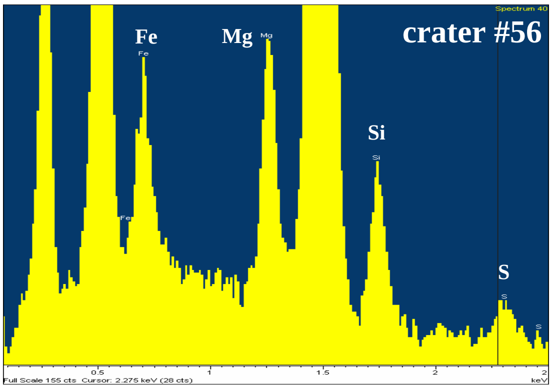

3.4. EDX scanning of large crater on foil 013N

EDX scanning was performed with an Oxford Instruments EDX system. We worked with an acceleration voltage of 20 kV and an integration time of 43.6 s per frame and acquired a maximum of 1000 frames per image. This results in an integration time of 12.1 hours. Image size was 512 x 336 pixels. In order to optimize the signal from the impactor residue the foil was tilted by 30 degrees. Additionally, for Si, O and Mg measurements, a second map was acquired after rotating the sample by 180 degrees to investigate also the opposite side of the crater wall (Fig. 7). Signal intensity was highest from the crater wall and part of the crater floor. However, most of the crater floor (cf. Fig. 8) is not visible for the x-ray detector due to geometric shadowing effects.

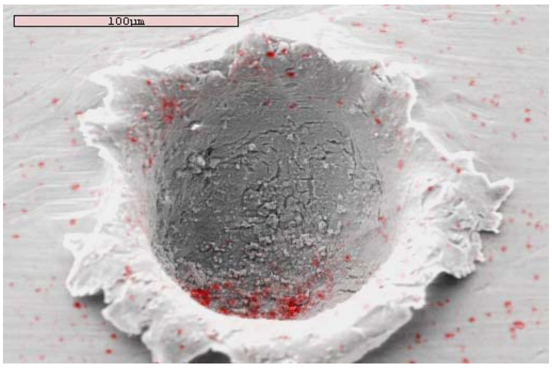

Fe (max. 113 counts)

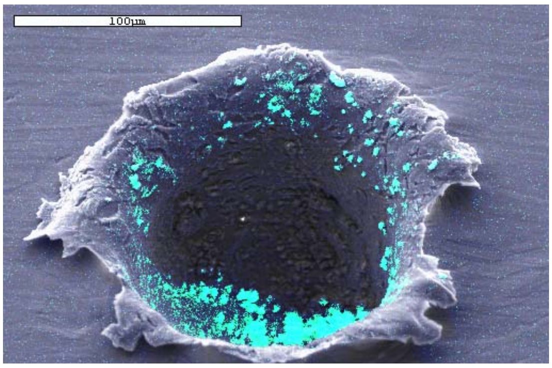

Mg (max. 87 counts)

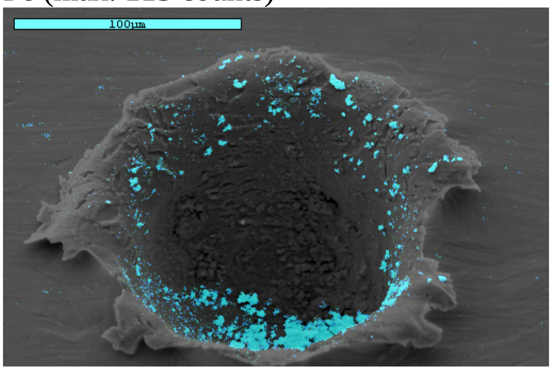

O (max. 68 counts)

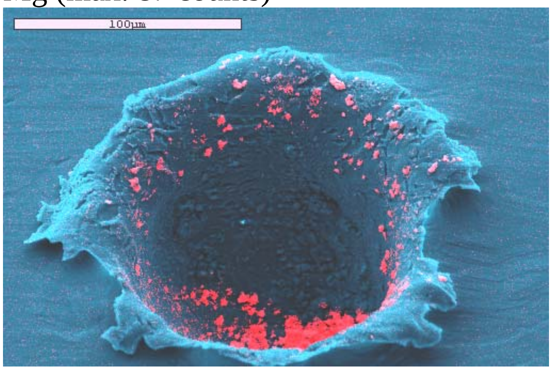

Si (max. 67 counts)

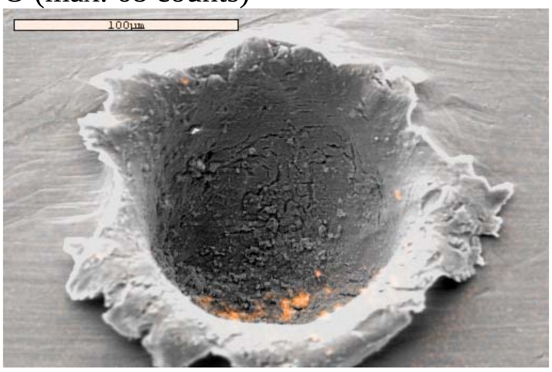

Na (max. 61 counts)

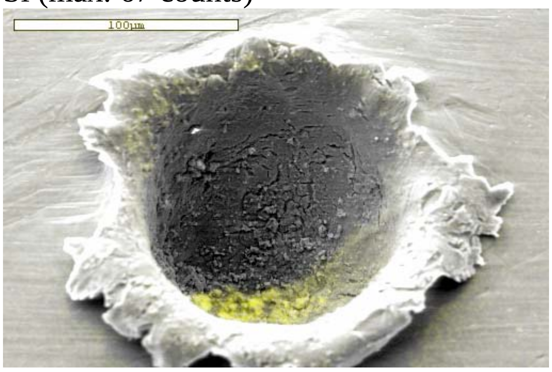

S (max. 50 counts)

Figure 7: EDX elemental maps of the residue in the large crater on foil 013N superimposed on SEM images acquired with a tilt angle of 30 degrees and an integration time of 12.1 hours.

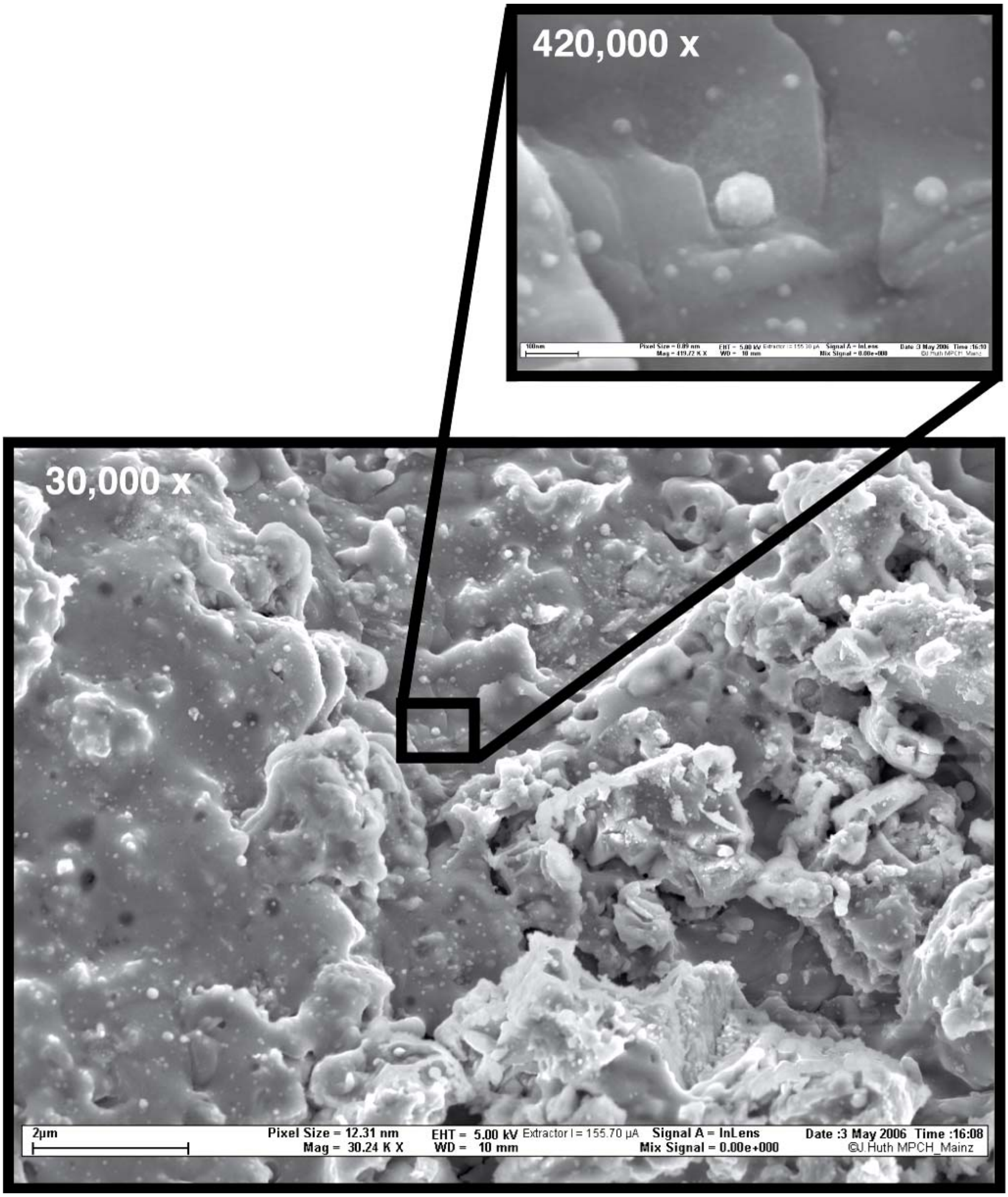

Figure 8: High-resolution SEM images of impact residue on the floor of the large crater on foil 013N. The scale bar is 2 µm on the lower image and 100 nm on the inset image above.

Appendix A

Crater	Size (nm)	X[1] (µm)	Y (µm)	Crater	Size (nm)	X (µm)	Y (µm)
044W				15	309	53948	23951
Region I:				16	306	54001	24108
2	710	44000	37460	17	428	53642	23259
3	710	43933	37460	18	953	53226	23295
				19	452	53286	23323
XY-UL[2]		44133	36525	20	454	53338	23568
XY-UR		43467	36525	21	286	53272	23575
XY-LL		44133	38195	22	737	53309	23609
XY-LR		43467	38195	23	399	53283	23648
				24	457	53238	23722
Region II:				25	352	53253	23744
4	630	38624	36451	26	366	53555	23607
5	450	38094	36519	27	416	53627	23856
6	160	38094	37653	28	940	53576	23995
7	220	38094	37653	29	369	53329	23926
8	180	38094	37653	30	404	53293	24016
9	370	37960	37720	31	589	53337	24034
10	230	37293	36422	32	356	53134	24285
11	290	37093	36822	33	264	53524	24364
12	320	37160	36956	34	464	53561	24577
13	990	37360	37756	35	324	53418	24457
14	510	37025	36421	36	491	53200	24598
15	350	36493	36355	37	308	53050	23148
16	690	36893	36556	38	268	53028	23136
17	320	37093	36689	39	386	52478	23084
18	340	36760	37223	40	589	53023	23197
19	410	36826	37556	41	305	53083	23202
				42	1092	52920	23279
XY-UL		38822	36319	43	320	52799	23243
XY-UR		36493	36319	44	606	52727	23218
XY-LL		38822	38023	45	471	52606	23197
XY-LR		36493	38023	46	436	52778	23455
				47	208	52879	23535
052N				48	450	52631	23676
5	276	54772	23157	49	389	52872	23813
6	385	54288	23225	50	421	52685	23843
7	365	54509	23369	51	389	52896	23894
8	335	54436	23479	52	510	53020	23923
9	553	54864	23839	53	399	52813	24160
10	931	54744	24126	54	474	53040	24291
11	442	54830	24353	55	709	52725	24300
12	374	54731	24067	56	490	51906	23346
13	352	53762	23533	57	367	52248	23391
14	476	53817	23917	58	346	52151	23520

Crater	Size (nm)	X (μm)	Y (μm)		Crater	Size (nm)	X (μm)	Y (μm)
59	349	51964	23740		105	400	50836	23306
60	425	52245	23838		106	586	50828	23257
61	131	52301	23885		107	430	50917	23210
62	230	52354	23888		108	278	50699	23152
63	332	52413	23909		109	271	51098	23302
64	321	52017	23913		110	281	50979	23664
65	114	52241	23977		111	182	50893	23649
66	427	52240	23978		112	129	50885	23641
67	334	52389	23995		113	341	50815	23621
68	380	52353	24145		114	769	51056	23754
69	350	52392	24186		115	301	50868	23832
70	177	52284	24201		116	357	50864	23910
71	560	52234	24195		117	388	50912	23934
72	238	52395	24270		118	373	51079	23988
73	290	52381	24262		119	258	51184	23980
74	349	52448	24324		120	449	51215	23994
75	373	51869	24568		121	236	51265	24045
76	419	52158	24269		122	483	51048	24069
77	262	51791	23058		123	282	51052	24343
78	301	51641	23064		124	725	50947	24440
79	292	51594	23170		125	357	51278	24568
80	657	51740	23264		126	1001	51212	24587
81	409	51508	23288		127	656	50682	23450
82	1348	51372	23284		129	1105	50435	23748
83	508	51428	23315		130	1517	50553	23981
84	287	51312	23332		131	459	50380	23325
85	474	51887	23338		132	363	50227	23379
86	541	51761	23494		133	484	50211	23112
87	276	51759	23594		134	733	50201	23131
88	400	51760	23603		135	322	50151	23508
89	294	51615	23703		136	485	50542	23504
90	329	51752	23768		137	459	50479	23624
91	586	51379	23869		138	325	50425	23872
92	193	51655	23880		139	272	50128	23918
93	377	51449	24093		140	446	50149	23838
94	349	51771	24220		141	521	50095	24069
95	389	51703	24412		142	456	50272	24072
96	1187	51556	24465		143	528	50157	24140
97	312	51444	24440		144	705	50092	24196
98	378	51496	24378		145	301	50675	24092
99	572	51535	24562		146	242	50570	24195
100	362	51851	24569		147	260	50551	24199
101	138	51169	23481		148	752	50473	24209
102	213	51276	23528		150	1266	50257	24273
103	267	50866	23516		151	216	50196	24440
104	307	50668	23442		152	388	50307	24623

Crater	Size (nm)	X (µm)	Y (µm)		Crater	Size (nm)	X (µm)	Y (µm)
153	447	50371	23591		Region II:			
154	398	50582	23477		8	457	40674	25373
155	793	49983	23214		9	377	40619	25373
156	466	49718	23305		10	536	40396	25317
157	219	49820	23236		11	255	40507	25317
158	1236	49548	23280		12	627	40452	25150
159	346	49963	23363		13	198	40452	25150
160	240	49717	23346		14	286	40284	25095
161	260	49484	23558		15	265	40284	25373
162	289	49953	23762		16	304	40284	25429
163	505	49838	23832		17	1110	40284	25540
164	345	49876	23890		18	633	40173	25262
165	363	49637	23870		19	271	40619	25484
166	551	50018	24065		20	570	40229	25150
167	260	50046	24446		21	439	40173	25095
168	365	49465	24288		22	400	40062	25206
169	322	49834	24160		24	587	40117	25373
170	455	49767	24153		25	712	40117	25429
171	245	49766	24149		26	475	39950	25485
172	219	49975	24124		27	1324	39839	25485
					28	519	40006	25540
XY-UL		54967	23049		29	361	40006	25540
XY-UR		49483	23047		30	336	39783	25429
XY-LL		54967	24686		31	279	39783	25373
XY-LR		49489	24683		32	432	39672	25373
					33	261	39672	25206
126W					34	488	39672	25150
1	270				35	611	39616	25429
2	370				36	480	39504	25318
					37	627	39282	25262
037N[3]					38	217	39449	25150
1	3810				39	336	39449	25150
					40	282	39449	25150
Region I:					41	263	39282	25095
2	316	41172	24596		42	409	39337	25485
3	409	40840	24596		43	581	39282	25485
4	940	40951	24707		44	287	39226	25429
5	223	41006	24928		45	915	39059	25039
6	272	41006	24928		46	556	38947	25095
7	856	40896	25039		47	691	39003	25095
56	1860	40675	25039		48	377	39114	25262
					49	487	39003	25373
XY-UL		41199	24514		50	591	38780	25373
XY-UR		40642	24514		51	251	38780	25318
XY-LL		41199	25071		52	216	38725	25262
XY-LR		40642	25071		53	404	38836	25206

Crater	Size (nm)	X (μm)	Y (μm)		Crater	Size (nm)	X (μm)	Y (μm)
54	344	38669	25039		XY-UL		40647	25011
55	387	38725	25485		XY-UR		38641	25011
					XY-LL		40647	25567
					XY-LR		38641	25567

[1]X, Y: coordinates of crater locations.
[2]XY-UL, -UR, -LL, -LR: coordinates of the corners of the scanned area.
[3]Crater coordinates are precise only within ±30 μm because of problems with the sample stage. More precise coordinates will be given later, if needed.

Appendix B

Crater No.	Mg [at%]	Si [at%]	S [at%]	Fe [at%]	Ni [at%]	O [at%]	others	Mineralogy, qualtitatively[1]
044W								
1								Silicate
2								Silicate + FeS
3								Silicate + FeS
4								Silicate + FeS
5								Silicate + FeS
6								Silicate
7								FeS
8								FeS + Silicate
9								Silicate + FeS
10								FeS
11								Silicate
12								Silicate + FeS
13								Silicate
052N								
1								Silicate + FeS
28								FeS
42								Silicate + FeS
44								FeS + Si
71								Silicate + FeS
96								Silicate
106								Silicate + FeS
114								Silicate
124								FeS + Silicate
130								Silicate
158								Silicate + FeS
037N								
4	16.1	15.2	0.0	6.4	0.0	62.3		Silicate
7	18.8	14.0	0.0	6.1	0.0	61.1		Silicate
8	17.9	19.5	0.0	2.4	0.0	60.2		Silicate
12	0.0	0.0	50.8	49.2	0.0	0.0		FeS
14	11.5	23.9	0.0	0.0	0.0	64.6	Ca	Silicate
	10.6	23.3	0.0	0.7	0.0	65.4	Ca	
	10.6	21.9	0.0	0.0	0.0	67.5	Ca	
18	0.0	0.0	58.9	31.1	9.9	0.0		(Fe-Ni)S
20	14.7	18.9	4.1	4.2	0.0	62.2		Silicate + FeS
25	0.0	0.0	58.5	41.5	0.0	0.0		FeS
27	19.1	20.0	0.0	1.5	0.0	59.4		Silicate
	14.9	23.1	0.0	1.0	0.0	61.0		
	17.4	21.2	0.0	1.3	0.0	60.0		
	20.5	16.5	0.0	3.5	0.0	59.5		
32	14.8	15.8	5.4	6.5	0.0	63.0		Silicate + FeS
35	10.6	5.9	12.0	15.6	0.0	67.9		Silicate + FeS

Crater No.	Mg [at%]	Si [at%]	S [at%]	Fe [at%]	Ni [at%]	O [at%]	others	Mineralogy, qualtitatively[1]
	11.0	15.3	8.9	8.5	0.0	65.2		
	15.2	18.7	2.8	4.1	0.0	61.9		
37	15.7	21.6	2.7	1.8	0.0	60.9		Silicate
	16.7	21.1	1.6	1.7	0.0	60.5		
	16.5	19.6	1.4	2.9	0.0	61.0		
39	12.7	9.4	12.8	12.1	0.0	65.8		Silicate + FeS
	10.5	7.7	13.7	14.3	4.1	67.5		
	10.7	9.1	13.4	13.2	8.6	67.0		
	13.6	12.4	18.0	9.5	0.0	64.5		
	13.6	15.9	10.8	6.9	0.0	63.6		
46	18.7	14.1	6.5	6.1	0.0	61.2		Silicate + FeS
	20.4	12.9	4.8	6.2	0.0	60.5		
	18.6	13.4	4.3	6.7	0.0	61.4		
47	14.8	12.7	10.4	8.8	0.0	63.7		Silicate + FeS
48	17.5	17.3	1.9	4.2	0.0	61.0		Silicate
	13.1	18.3	2.7	5.3	0.0	63.3		
49	19.4	21.9	0.0	0.0	0.0	58.7		Silicate
50	16.3	10.7	9.6	9.6	0.0	63.4		Silicate + FeS
	17.9	14.7	1.6	3.0	0.0	64.3		
56	23.0	19.0	0.0	0.6	0.0	57.4		Silicate + FeS
	17.4	21.4	0.0	1.1	0.0	60.2	Na	
	15.5	12.3	2.8	8.5	0.0	63.7	Na	
	16.8	14.5	2.4	6.6	0.0	62.1		
	15.2	15.2	3.5	6.8	0.0	62.9		
	6.6	29.2	0.0	0.0	0.0	64.2		

[1]If more than one mineral type is given, the first one is more abundant than the second one.